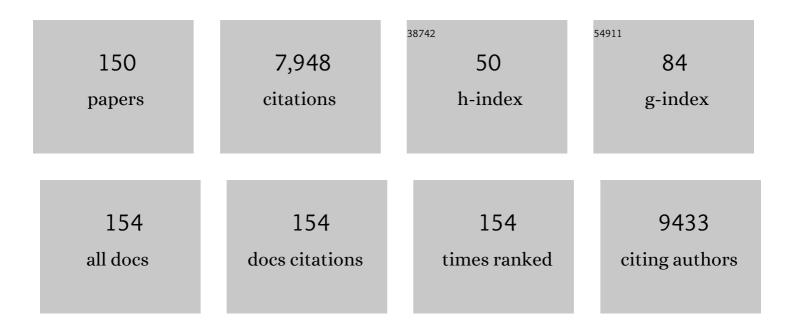
## Seong Chan Jun

List of Publications by Year in descending order

Source: https://exaly.com/author-pdf/950754/publications.pdf Version: 2024-02-01



#	Article	IF	CITATIONS
1	Hierarchical MnCo-layered double hydroxides@Ni(OH) <sub>2</sub> core–shell heterostructures as advanced electrodes for supercapacitors. Journal of Materials Chemistry A, 2017, 5, 1043-1049.	10.3	296
2	Effect of cation substitution on the pseudocapacitive performance of spinel cobaltite MCo <sub>2</sub> O <sub>4</sub> (M = Mn, Ni, Cu, and Co). Journal of Materials Chemistry A, 2018, 6, 10674-10685.	10.3	266
3	Recent Advances in Vanadiumâ€Based Aqueous Rechargeable Zincâ€Ion Batteries. Advanced Energy Materials, 2020, 10, 2000477.	19.5	265
4	Structural engineering and surface modification of MOF-derived cobalt-based hybrid nanosheets for flexible solid-state supercapacitors. Energy Storage Materials, 2020, 32, 167-177.	18.0	228
5	Hierarchical manganese cobalt sulfide core–shell nanostructures for high-performance asymmetric supercapacitors. Journal of Power Sources, 2017, 342, 629-637.	7.8	221
6	New insight into the effect of fluorine doping and oxygen vacancies on electrochemical performance of Co2MnO4 for flexible quasi-solid-state asymmetric supercapacitors. Energy Storage Materials, 2019, 22, 384-396.	18.0	189
7	Challenges and Strategies toward Cathode Materials for Rechargeable Potassiumâ€lon Batteries. Advanced Materials, 2021, 33, e2004689.	21.0	188
8	Unlocking the Potential of Oxygen-Deficient Copper-Doped Co <sub>3</sub> O <sub>4</sub> Nanocrystals Confined in Carbon as an Advanced Electrode for Flexible Solid-State Supercapacitors. ACS Energy Letters, 2021, 6, 3011-3019.	17.4	173
9	Enhanced Supercapacitive Performance of Chemically Grown Cobalt–Nickel Hydroxides on Three-Dimensional Graphene Foam Electrodes. ACS Applied Materials & Interfaces, 2014, 6, 2450-2458.	8.0	164
10	Recent Advances and Perspectives of Battery-Type Anode Materials for Potassium Ion Storage. ACS Nano, 2021, 15, 18931-18973.	14.6	160
11	Highâ€Performance Flexible Quasiâ€Solidâ€State Supercapacitors Realized by Molybdenum Dioxide@Nitrogenâ€Doped Carbon and Copper Cobalt Sulfide Tubular Nanostructures. Advanced Science, 2018, 5, 1800733.	11.2	156
12	Phosphorous-containing oxygen-deficient cobalt molybdate as an advanced electrode material for supercapacitors. Energy Storage Materials, 2019, 19, 186-196.	18.0	145
13	Conceptual design of three-dimensional CoN/Ni <sub>3</sub> N-coupled nanograsses integrated on N-doped carbon to serve as efficient and robust water splitting electrocatalysts. Journal of Materials Chemistry A, 2018, 6, 4466-4476.	10.3	143
14	High-performance gas sensor array for indoor air quality monitoring: the role of Au nanoparticles on WO <sub>3</sub> , SnO <sub>2</sub> , and NiO-based gas sensors. Journal of Materials Chemistry A, 2021, 9, 1159-1167.	10.3	141
15	Dual-defect surface engineering of bimetallic sulfide nanotubes towards flexible asymmetric solid-state supercapacitors. Journal of Materials Chemistry A, 2020, 8, 24053-24064.	10.3	133
16	Effect of fluorine doping and sulfur vacancies of CuCo2S4 on its electrochemical performance in supercapacitors. Chemical Engineering Journal, 2020, 390, 124643.	12.7	132
17	Carbonaceous Anode Materials for Non-aqueous Sodium- and Potassium-Ion Hybrid Capacitors. ACS Energy Letters, 2021, 6, 4127-4154.	17.4	129
18	Binder-free cobalt phosphate one-dimensional nanograsses as ultrahigh-performance cathode material for hybrid supercapacitor applications. Journal of Power Sources, 2018, 373, 211-219.	7.8	127

#	Article	IF	CITATIONS
19	Nanostructured pseudocapacitive materials decorated 3D graphene foam electrodes for next generation supercapacitors. Nanoscale, 2015, 7, 6999-7021.	5.6	124
20	Honeycomb-Like Interconnected Network of Nickel Phosphide Heteronanoparticles with Superior Electrochemical Performance for Supercapacitors. ACS Applied Materials & Interfaces, 2017, 9, 21829-21838.	8.0	123
21	Scalable fabrication of micron-scale graphene nanomeshes for high-performance supercapacitor applications. Energy and Environmental Science, 2016, 9, 1270-1281.	30.8	122
22	Amorphous Phosphorus-Incorporated Cobalt Molybdenum Sulfide on Carbon Cloth: An Efficient and Stable Electrocatalyst for Enhanced Overall Water Splitting over Entire pH Values. ACS Applied Materials & Interfaces, 2017, 9, 37739-37749.	8.0	122
23	Review on Recent Progress in the Development of Tungsten Oxide Based Electrodes for Electrochemical Energy Storage. ChemSusChem, 2020, 13, 11-38.	6.8	121
24	Controlled electrochemical growth of Co(OH) <sub>2</sub> flakes on 3D multilayered graphene foam for high performance supercapacitors. Journal of Materials Chemistry A, 2014, 2, 19075-19083.	10.3	117
25	Chemiresistive Electronic Nose toward Detection of Biomarkers in Exhaled Breath. ACS Applied Materials & Interfaces, 2016, 8, 20969-20976.	8.0	113
26	Stacked Porous Iron-Doped Nickel Cobalt Phosphide Nanoparticle: An Efficient and Stable Water Splitting Electrocatalyst. ACS Sustainable Chemistry and Engineering, 2018, 6, 6146-6156.	6.7	113
27	Atomicâ€Level Platinum Filling into Niâ€Vacancies of Dualâ€Deficient NiO for Boosting Electrocatalytic Hydrogen Evolution. Advanced Energy Materials, 2022, 12, .	19.5	110
28	Controllable sulfuration engineered NiO nanosheets with enhanced capacitance for high rate supercapacitors. Journal of Materials Chemistry A, 2017, 5, 4543-4549.	10.3	105
29	Nanomechanical hydrogen sensing. Applied Physics Letters, 2005, 86, 143104.	3.3	103
30	Static and Dynamic Performance of Complementary Inverters Based on Nanosheet α-MoTe <sub>2</sub> <i>p</i> -Channel and MoS <sub>2</sub> <i>n</i> -Channel Transistors. ACS Nano, 2016, 10, 1118-1125.	14.6	98
31	Electrothermal tuning of Al–SiC nanomechanical resonators. Nanotechnology, 2006, 17, 1506-1511.	2.6	96
32	Enhanced Symmetric Supercapacitive Performance of Co(OH)2 Nanorods Decorated Conducting Porous Graphene Foam Electrodes. Electrochimica Acta, 2014, 129, 334-342.	5.2	91
33	Phosphorus Regulated Cobalt Oxide@Nitrogenâ€Doped Carbon Nanowires for Flexible Quasiâ€Solidâ€State Supercapacitors. Small, 2020, 16, e1906458.	10.0	90
34	Vertical and In-Plane Current Devices Using NbS <sub>2</sub> /n-MoS <sub>2</sub> van der Waals Schottky Junction and Graphene Contact. Nano Letters, 2018, 18, 1937-1945.	9.1	86
35	Phosphorusâ€Doped Graphene Oxide Layer as a Highly Efficient Flame Retardant. Chemistry - A European Journal, 2015, 21, 15480-15485.	3.3	85
36	Realizing Superior Redox Kinetics of Hollow Bimetallic Sulfide Nanoarchitectures by Defectâ€Induced Manipulation toward Flexible Solidâ€State Supercapacitors. Small, 2022, 18, e2104507.	10.0	85

#	Article	IF	CITATIONS
37	Epoxy to Carbonyl Group Conversion in Graphene Oxide Thin Films: Effect on Structural and Luminescent Characteristics. Journal of Physical Chemistry C, 2012, 116, 19010-19017.	3.1	83
38	Phosphorus dual-site driven CoS <sub>2</sub> @S, N co-doped porous carbon nanosheets for flexible quasi-solid-state supercapacitors. Journal of Materials Chemistry A, 2019, 7, 26618-26630.	10.3	82
39	Phosphorusâ€Mediated MoS <sub>2</sub> Nanowires as a Highâ€Performance Electrode Material for Quasiâ€Solidâ€State Sodiumâ€Ion Intercalation Supercapacitors. Small, 2019, 15, e1803984.	10.0	81
40	Redox Additive-Improved Electrochemically and Structurally Robust Binder-Free Nickel Pyrophosphate Nanorods as Superior Cathode for Hybrid Supercapacitors. ACS Applied Materials & Interfaces, 2018, 10, 8045-8056.	8.0	75
41	Layered manganese metal-organic framework with high specific and areal capacitance for hybrid supercapacitors. Chemical Engineering Journal, 2020, 387, 122982.	12.7	74
42	Cobalt carbonate hydroxides as advanced battery-type materials for supercapatteries: Influence of morphology on performance. Electrochimica Acta, 2018, 259, 1037-1044.	5.2	70
43	A facile synthesis of hierarchical α-MnO2 nanofibers on 3D-graphene foam for supercapacitor application. Materials Letters, 2014, 119, 135-139.	2.6	68
44	PolyHIPE Derived Freestanding 3D Carbon Foam for Cobalt Hydroxide Nanorods Based High Performance Supercapacitor. Scientific Reports, 2016, 6, 35490.	3.3	67
45	Multicolor emissive carbon dot with solvatochromic behavior across the entire visible spectrum. Carbon, 2020, 156, 110-118.	10.3	64
46	Direct growth of WO3 nanostructures on multi-walled carbon nanotubes for high-performance flexible all-solid-state asymmetric supercapacitor. Electrochimica Acta, 2019, 308, 231-242.	5.2	63
47	Two-dimensional MXenes for electrochemical energy storage applications. Journal of Materials Chemistry A, 2022, 10, 1105-1149.	10.3	63
48	Facile approach to synthesize highly fluorescent multicolor emissive carbon dots via surface functionalization for cellular imaging. Journal of Colloid and Interface Science, 2018, 513, 505-514.	9.4	62
49	A binder free synthesis of 1D PANI and 2D MoS <sub>2</sub> nanostructured hybrid composite electrodes by the electrophoretic deposition (EPD) method for supercapacitor application. RSC Advances, 2016, 6, 101592-101601.	3.6	57
50	Clean transfer of graphene and its effect on contact resistance. Applied Physics Letters, 2013, 103, .	3.3	56
51	3D yolk–shell NiGa <sub>2</sub> S <sub>4</sub> microspheres confined with nanosheets for high performance supercapacitors. Journal of Materials Chemistry A, 2017, 5, 6292-6298.	10.3	52
52	Contact Effect of ReS <sub>2</sub> /Metal Interface. ACS Applied Materials & Interfaces, 2017, 9, 26325-26332.	8.0	50
53	Layer dependence and gas molecule absorption property in MoS2 Schottky diode with asymmetric metal contacts. Scientific Reports, 2015, 5, 10440.	3.3	49
54	All-redox solid-state supercapacitor with cobalt manganese oxide@bimetallic hydroxides and vanadium nitride@nitrogen-doped carbon electrodes. Chemical Engineering Journal, 2021, 405, 127029.	12.7	49

#	Article	IF	CITATIONS
55	An asymmetric supercapacitor with excellent cycling performance realized by hierarchical porous NiGa <sub>2</sub> O <sub>4</sub> nanosheets. Journal of Materials Chemistry A, 2017, 5, 19046-19053.	10.3	48
56	Highly Dispersed Pt Clusters on F-Doped Tin(IV) Oxide Aerogel Matrix: An Ultra-Robust Hybrid Catalyst for Enhanced Hydrogen Evolution. ACS Nano, 2022, 16, 1625-1638.	14.6	48
57	Humidityâ€Tolerant Singleâ€Stranded DNAâ€Functionalized Graphene Probe for Medical Applications of Exhaled Breath Analysis. Advanced Functional Materials, 2017, 27, 1700068.	14.9	47
58	Self-assembled bimetallic cobalt–manganese metal–organic framework as a highly efficient, robust electrode for asymmetric supercapacitors. Electrochimica Acta, 2020, 335, 135327.	5.2	46
59	Post-heating effects on the physical and electrochemical capacitive properties of reduced graphene oxide paper. Journal of Materials Chemistry A, 2014, 2, 5077.	10.3	44
60	Substrate and buffer layer effect on the structural and optical properties of graphene oxide thin films. RSC Advances, 2013, 3, 5926.	3.6	43
61	Metal–organic-framework-derived hierarchical Co/CoP-decorated nanoporous carbon polyhedra for robust high-energy storage hybrid supercapacitors. Dalton Transactions, 2020, 49, 1157-1166.	3.3	42
62	Fabrication of ultra-high energy and power asymmetric supercapacitors based on hybrid 2D MoS <sub>2</sub> /graphene oxide composite electrodes: a binder-free approach. RSC Advances, 2016, 6, 43261-43271.	3.6	41
63	Graphene-Iodine Nanocomposites: Highly Potent Bacterial Inhibitors that are Bio-compatible with Human Cells. Scientific Reports, 2016, 6, 20015.	3.3	38
64	Potentiodynamic polarization assisted phosphorus-containing amorphous trimetal hydroxide nanofibers for highly efficient hybrid supercapacitors. Journal of Materials Chemistry A, 2020, 8, 5721-5733.	10.3	38
65	All-solid-state flexible asymmetric micro supercapacitors based on cobalt hydroxide and reduced graphene oxide electrodes. RSC Advances, 2016, 6, 43844-43854.	3.6	37
66	Nickel hydroxide/chemical vapor deposition-grown graphene/nickel hydroxide/nickel foam hybrid electrode for high performance supercapacitors. Electrochimica Acta, 2019, 297, 479-487.	5.2	37
67	Tunable wide blue photoluminescence with europium decorated graphene. Journal of Materials Chemistry C, 2015, 3, 4030-4038.	5.5	36
68	Radio frequency based label-free detection of glucose. Biosensors and Bioelectronics, 2014, 54, 141-145.	10.1	34
69	Unconventional Terahertz Carrier Relaxation in Graphene Oxide: Observation of Enhanced Auger Recombination Due to Defect Saturation. ACS Nano, 2014, 8, 2486-2494.	14.6	33
70	Efficient Direct Reduction of Graphene Oxide by Silicon Substrate. Scientific Reports, 2015, 5, 12306.	3.3	32
71	High-concentration dispersions of exfoliated MoS2 sheets stabilized by freeze-dried silk fibroin powder. Nano Research, 2016, 9, 1709-1722.	10.4	31
72	Controlling the luminescence emission from palladium grafted graphene oxide thin films via reduction. Nanoscale, 2013, 5, 5620.	5.6	30

#	Article	IF	CITATIONS
73	Facile hydrothermal synthesis of carbon-coated cobalt ferrite spherical nanoparticles as a potential negative electrode for flexible supercapattery. Journal of Colloid and Interface Science, 2018, 513, 480-488.	9.4	30
74	Enhanced Non-enzymatic amperometric sensing of glucose using Co(OH)2 nanorods deposited on a three dimensional graphene network as an electrode material. Mikrochimica Acta, 2016, 183, 2473-2479.	5.0	29
75	Electrically focus-tuneable ultrathin lens for high-resolution square subpixels. Light: Science and Applications, 2020, 9, 98.	16.6	29
76	Surface plasmon enhancement of photoluminescence in photo-chemically synthesized graphene quantum dot and Au nanosphere. Nano Research, 2016, 9, 1866-1875.	10.4	28
77	Sensitivity Enhancement of Bead-based Electrochemical Impedance Spectroscopy (BEIS) biosensor by electric field-focusing in microwells. Biosensors and Bioelectronics, 2016, 85, 16-24.	10.1	28
78	Two-dimensional electronic devices modulated by the activation of donor-like states in boron nitride. Nanoscale, 2020, 12, 18171-18179.	5.6	28
79	Radio-frequency characteristics of graphene oxide. Applied Physics Letters, 2010, 97, .	3.3	27
80	Reduced graphene oxide enwrapped phosphors for long-term thermally stable phosphor converted white light emitting diodes. Scientific Reports, 2016, 6, 33993.	3.3	27
81	Passive electrical properties of multi-walled carbon nanotubes up to 0.1 THz. New Journal of Physics, 2007, 9, 265-265.	2.9	26
82	Top and back gate molybdenum disulfide transistors coupled for logic and photo-inverter operation. Journal of Materials Chemistry C, 2014, 2, 8023-8028.	5.5	26
83	Few-layered α-MoTe <sub>2</sub> Schottky junction for a high sensitivity chemical-vapour sensor. Journal of Materials Chemistry C, 2018, 6, 10714-10722.	5.5	25
84	An unexpected phase-transformation of cobalt–vanadium layered double hydroxides toward high energy density hybrid supercapacitor. Journal of Power Sources, 2021, 486, 229341.	7.8	25
85	Terahertz and optical study of monolayer graphene processed by plasma oxidation. Applied Physics Letters, 2013, 102, .	3.3	24
86	A MEMS ultrasound stimulation system for modulation of neural circuits with high spatial resolution in vitro. Microsystems and Nanoengineering, 2019, 5, 28.	7.0	24
87	Nitrogen-doped carbon integrated nickel–cobalt metal phosphide marigold flowers as a high capacity electrode for hybrid supercapacitors. CrystEngComm, 2020, 22, 6360-6370.	2.6	23
88	A systematic approach to achieve high energy density hybrid supercapacitors based on Ni–Co–Fe hydroxide. Electrochimica Acta, 2020, 353, 136578.	5.2	22
89	2D-on-2D core–shell Co <sub>3</sub> (PO <sub>4</sub> ) <sub>2</sub> stacked micropetals@Co <sub>2</sub> Mo <sub>3</sub> O <sub>8</sub> nanosheets and binder-free 2D CNT–Ti <sub>3</sub> C <sub>2</sub> T <sub><i>X</i>&gt; Sub&gt;3€"MXene electrodes for high-energy solid-state flexible supercapacitors, lournal of Materials Chemistry A, 2021, 9, 26135-26148.</sub>	10.3	22
90	A reversible and stable doping technique to invert the carrier polarity of MoTe2. Nanotechnology, 2021, 32, 285701.	2.6	21

#	Article	IF	CITATIONS
91	Terahertz, optical, and Raman signatures of monolayer graphene behavior in thermally reduced graphene oxide films. Journal of Applied Physics, 2013, 113, .	2.5	20
92	Tunable near white light photoluminescence of lanthanide ion (Dy3+, Eu3+and Tb3+) doped DNA lattices. RSC Advances, 2015, 5, 55839-55846.	3.6	19
93	Graphene Derivative As a Highly Efficient Nitrosonium Source: A Reusable Catalyst for Diazotization and Coupling Reaction. ChemistrySelect, 2016, 1, 6933-6940.	1.5	18
94	Temperature influenced chemical growth of hydrous copper oxide/hydroxide thin film electrodes for high performance supercapacitors. Journal of Alloys and Compounds, 2017, 701, 1009-1018.	5.5	18
95	Structural, chemical, and electrical parameters of Au/MoS2/n-GaAs metal/2D/3D hybrid heterojunction. Journal of Colloid and Interface Science, 2019, 550, 48-56.	9.4	18
96	Impact of different nanostructures of a PEDOT decorated 3D multilayered graphene foam by chemical methods on supercapacitive performance. RSC Advances, 2015, 5, 107864-107871.	3.6	17
97	Sensitivity Enhancement in Nickel Hydroxide/3Dâ€Graphene as Enzymeless Glucose Detection. Electroanalysis, 2015, 27, 2363-2370.	2.9	16
98	Interfacial Assembled CeO <sub>2–<i>x</i></sub> /Co@N-Doped Carbon Hollow Nanohybrids for High-Performance Lithium–Sulfur Batteries. ACS Sustainable Chemistry and Engineering, 2021, 9, 14451-14460.	6.7	16
99	Review of contact-resistance analysis in nano-material. Journal of Mechanical Science and Technology, 2018, 32, 539-547.	1.5	15
100	Hydrous nickel sulphide nanoparticle decorated 3D graphene foam electrodes for enhanced supercapacitive performance of an asymmetric device. New Journal of Chemistry, 2018, 42, 20123-20130.	2.8	15
101	Hierarchically designed 3D Cu3N@Ni3N porous nanorod arrays: An efficient and robust electrode for high-energy solid-state hybrid supercapacitors. Applied Materials Today, 2021, 22, 100951.	4.3	15
102	Construction of hierarchical nickel cobalt sulfide@manganese oxide nanoarrays@nanosheets <scp>coreâ€shell</scp> electrodes for highâ€performance electrochemical asymmetric supercapacitor. International Journal of Energy Research, 2022, 46, 5250-5259.	4.5	14
103	A Reduced Graphene Oxide Based Radio Frequency Glucose Sensing Device Using Multi-Dimensional Parameters. Micromachines, 2016, 7, 136.	2.9	13
104	Environmentally benign and cost-effective synthesis of water soluble red light emissive gold nanoclusters: selective and ultra-sensitive detection of mercuric ions. New Journal of Chemistry, 2019, 43, 900-906.	2.8	13
105	Simultaneous integration of low-level rhenium (Re) doping and nitrogen-functionalized 3D carbon backbone into nickel-iron hydroxide (NiFeOH) to amplify alkaline water electrolysis at high current densities. Chemical Engineering Journal, 2022, 435, 135184.	12.7	13
106	Artificial Rod and Cone Photoreceptors with Human‣ike Spectral Sensitivities. Advanced Materials, 2018, 30, e1706764.	21.0	12
107	Multi-heterostructured spin-valve junction of vertical FLG/MoSe2/FLG. APL Materials, 2020, 8, .	5.1	11
108	Highly Desirable Platform for Efficient Hydrogen Generation: Electrodeposited CoP on N-Doped Vertical Graphene. ACS Applied Energy Materials, 2021, 4, 5697-5705.	5.1	11

#	Article	IF	CITATIONS
109	Development of directly grownâ€graphene–silicon Schottky barrier solar cell using coâ€doping technique. International Journal of Energy Research, 2022, 46, 11510-11522.	4.5	11
110	Surface roughness effects on the frequency tuning performance of a nanoelectromechanical resonator. Nanoscale Research Letters, 2013, 8, 270.	5.7	10
111	Resonance Properties of 3C-SiC Nanoelectromechanical Resonator in Room-Temperature Magnetomotive Transduction. IEEE Electron Device Letters, 2009, 30, 1042-1044.	3.9	9
112	Electrothermal noise analysis in frequency tuning of nanoresonators. Solid-State Electronics, 2008, 52, 1388-1393.	1.4	8
113	Enhanced nonlinear optical characteristics of copper-ion-doped double crossover DNAs. Nanoscale, 2015, 7, 18089-18095.	5.6	8
114	Cu <sub>2</sub> Oâ^'Cu <sub>2</sub> Se Mixedâ€Phase Nanoflake Arrays: pHâ€Universal Hydrogen Evolution Reactions with Ultralow Overpotential. ChemElectroChem, 2019, 6, 5014-5021.	3.4	8
115	Nonlinear characteristics in radio frequency nanoelectromechanical resonators. New Journal of Physics, 2010, 12, 043023.	2.9	7
116	Carrier scattering in quasi-free standing graphene on hexagonal boron nitride. Nanoscale, 2017, 9, 15934-15944.	5.6	7
117	Carrier Transport Properties of MoS2 Asymmetric Gas Sensor Under Charge Transfer-Based Barrier Modulation. Nanoscale Research Letters, 2018, 13, 265.	5.7	6
118	Bio-inspired interface engineering of Ag2O rooted on Au, Ni-modified filter paper for highly robust Zn–Ag2O batteries. Journal of Colloid and Interface Science, 2022, 623, 744-751.	9.4	6
119	Microwave transmission in graphene oxide. Nanotechnology, 2013, 24, 015201.	2.6	5
120	Biotin-streptavidin detection with a graphene-oxide supported radio-frequency resonator. Applied Physics Letters, 2013, 102, .	3.3	5
121	Detection of Retinitis Pigmentosa by Differential Interference Contrast Microscopy. PLoS ONE, 2014, 9, e97170.	2.5	5
122	Fundamental monomeric biomaterial diagnostics by radio frequency signal analysis. Biosensors and Bioelectronics, 2016, 82, 255-261.	10.1	5
123	Phonon-assisted carrier transport through a lattice-mismatched interface. NPG Asia Materials, 2019, 11, .	7.9	5
124	Focusâ€īunable Planar Lenses by Controlled Carriers over Exciton. Advanced Optical Materials, 2021, 9, 2001526.	7.3	5
125	Nonlinearity Control of Nanoelectromechanical Resonators. IEEE Electron Device Letters, 2012, 33, 1489-1491.	3.9	4
126	Flexible radio frequency interconnect of reduced graphene oxide. 2D Materials, 2018, 5, 035030.	4.4	4

#	Article	IF	CITATIONS
127	Impedance Variation on Lattice Misoriented Few-Layer Graphene Via Layer Decoupling. IEEE Nanotechnology Magazine, 2019, 18, 55-61.	2.0	4
128	Modulation of Magnetoresistance Polarity in BLC/SL-MoSe2 Heterostacks. Nanoscale Research Letters, 2020, 15, 136.	5.7	4
129	Evaluation of 3C-SiC Nanomechanical Resonators Using Room Temperature Magnetomotive Transduction. , 0, , .		3
130	Observation of scattering parameters for bandgap-tuned graphene oxide under 488Ânm illumination. Carbon, 2016, 109, 453-460.	10.3	3
131	Phosphorus-Mediated MoS2 : Phosphorus-Mediated MoS2 Nanowires as a High-Performance Electrode Material for Quasi-Solid-State Sodium-Ion Intercalation Supercapacitors (Small 4/2019). Small, 2019, 15, 1970026.	10.0	3
132	Graphene based NO <inf>2</inf> gas sensor. , 2010, , .		2
133	Mechanical Properties Changes During Electrothermal RF Tuning in a Nanoelectromechanical Resonator. IEEE Nanotechnology Magazine, 2013, 12, 596-600.	2.0	2
134	Dipole-assisted carrier transport in bis(trifluoromethane) sulfonamide-treated O-ReS2 field-effect transistor. Nano Research, 2021, 14, 2207-2214.	10.4	2
135	Facile Chemical Growth of Cu(OH) <sub>2</sub> Thin Film Electrodes for High Performance Supercapacitors. KEPCO Journal on Electric Power and Energy, 2015, 1, 175-180.	0.1	2
136	Microwave transmission characteristics of ZnO nanowire. Electronics Letters, 2012, 48, 1073-1074.	1.0	1
137	Observation of photoreceptor with retinitis pigmentosa by differential interference contrast microscopy. , 2013, , .		1
138	Determination of the molecular assembly of actin and actin-binding proteins using photoluminescence. Colloids and Surfaces B: Biointerfaces, 2018, 169, 462-469.	5.0	1
139	Preparation of graphene sponge with mechanical stability for compressible supercapacitor electrode. JMST Advances, 2019, 1, 81-87.	1.9	1
140	RF Characterization of Multi-walled carbon nanotube and ZnO film. , 2011, , .		0
141	Asbestos concentration measurement using Differential Interference Contrast microscopy. , 2012, , .		0
142	Terahertz study of reduced graphene oxide. , 2012, , .		0
143	Frontispiece: Phosphorus-Doped Graphene Oxide Layer as a Highly Efficient Flame Retardant. Chemistry - A European Journal, 2015, 21, n/a-n/a.	3.3	0
			_

Photoreceptors: Artificial Rod and Cone Photoreceptors with Human-Like Spectral Sensitivities (Adv.) Tj ETQq0 0 0 rgBT /Overlock 10 Tf 21.0

#	Article	IF	CITATIONS
145	Imaging and Differentiation of Retinal Ganglion Cells in Ex Vivo Experimental Optic Nerve Degeneration by Differential Interference Contrast Microscopy. Current Eye Research, 2019, 44, 760-769.	1.5	0
146	Energyâ€Dependent Spectral Analysis of Photonâ€Assisted Carrier Transport at Resonance in Graphene Oxide. Advanced Optical Materials, 2019, 7, 1800861.	7.3	0
147	Hysteresis control of nanoelectromechanical resonator with electrothermal power. Electronics Letters, 2014, 50, 1961-1963.	1.0	0
148	Preparation of Disordered Carbon Anode By Mechanical Method for Sodium Ion Battery. ECS Meeting Abstracts, 2018, , .	0.0	0
149	A Binder-Free Snowflake Grown Microcube Prussian Blue Particles As Possible Electrode for Supercapacitor and Sodium Ion Battery Applications. ECS Meeting Abstracts, 2018, , .	0.0	0
150	Inner-Constructed Growth Approach to Fabricate Integrated Chemical Vapor Deposition-Grown Graphene/Ni(OH)2/Ni Foam As an Advanced Electrode for Supercapacitors. ECS Meeting Abstracts, 2018, , .	0.0	0